



Rounded square ring resonator based add drop filter for WDM applications using two dimensional photonic crystals

Massoudi Radhouene¹ · V. R. Balaji² · Monia Najjar^{1,3} · S. Robinson⁴ · Vijay Janyani⁵ · M. Murugan⁶

Received: 22 October 2020 / Accepted: 17 April 2021 / Published online: 3 May 2021
© The Author(s), under exclusive licence to Springer Science+Business Media, LLC, part of Springer Nature 2021

Abstract

In this paper, Two Dimensional Photonic Crystals based Add Drop filter (ADF) is designed for DWDM applications. The existing work concentrates in Coarse Wavelength Division Multiplexing and few filters reported for DWDM with non-uniform channel spacing, and low quality factor. The proposed ADF enhances the quality factor using Rounded Square Ring Resonator (RSRR) for ensuring efficient bandwidth in supporting WDM systems. The design consists of bus waveguide, drop waveguide and RSRR with inner quasi-square ring in the square lattice. The dielectric constant of the Si rod is 11.68 which are hosted in the air. The line defect is created by removing 4 rods (Quasi ring) in the center of the inner square ring. The line defect in the ring resonator is used to reduce the radiation field components surrounded by the resonator. The performance parameters of ADF are investigated using 2D Finite Difference Time Domain algorithm. The proposed ADF drops a channel at 1636.2 nm, with the bandwidth of 0.7 nm, high quality factor of 2337, and the dropping efficiency of about 100%. The size of the device is $412.76 \mu\text{m}^2$. It is highly sufficient to support WDM systems for future Photonic Integrated Circuits (PIC). Further, the impact of functional parameters such as transmission efficiency, quality factor, bandwidth are investigated by varying the structural parameters, namely, adjacent rod radius, scatterer rod radius, coupling rod radius, lattice constant, inner rod radius and rod radius.

Keywords Quality factor · Ring resonator · Add drop filter · Photonic crystal · Photonic band gap

1 Introduction

Optical fiber communication sends the information with the pulses of light with less Bit Error Rate (BER) and high Signal to Noise Ratio (SNR) compared with the Radio Frequency (RF) communication. In optical fiber communication, the Single Mode Fiber (SMF) transfers the light for long distance and reaches the receiver end and the required

✉ V. R. Balaji
photonics.material@gmail.com

Extended author information available on the last page of the article

wavelength is dropped and added using the Add Drop Filter (ADF). Existing ADF are realized by Fabry–Perot cavity (Tran et al. 1996), gratings (Kersey et al. 1993), interferometers (Wooten et al. 1996) and microwave ring resonator (Sun et al. 2011). Nevertheless, this technology has limits in crosstalk, with low quality factor, more bending loss, low speed, and footprint in millimeter. The Photonic technology reduces the limitations and supports the ultra-high speed information processing, on nanoscale devices for Photonic Integrated Circuits.

The Photonic Crystal (PC) is a man-made artificial crystal, made of periodic dielectric material in space, acts as a potential barrier for the electromagnetic waves (Joannopoulos et al. 1997a, b). The PC allows and forbids certain waves to design any applications within the structure. The Photonic Band Gap (PBG) is a needed property in the PC. The incident light in PBG cannot propagate in the crystal, however, the light can be allowed to propagate by breaking the periodicity in the PC. By introducing the defects in the PC, it allows the electromagnetic waves to confine strongly in the periodic structure. The defect is classified as line defect for designing waveguides and point defect for the resonator.

The kind of PC classified as one-dimensional (1D). The 1D reported by Rayleigh (1887), but it took another 10 decades to introduce the 2D and 3DPC by Thomas Krauss. The 2DPC provides complete PBG compared with a 1DPC to provide high speed information processing. Also, the 2D fabrication is simple compared with 3DPC. Therefore, the 2DPC is a better choice for designing optical devices as it offers nano size, complete PBG and better light manipulation to integrate in PIC. Using 2DPC, There are many optical devices are reported, namely, LASER (Meier et al. 1999), filter (Fan et al. 1998), sensor (Fenzl et al. 2014), demultiplexer (Balaji et al. 2016), logic gates (Zhang et al. 2007), encoder (Mehdizadeh et al. 2016), Micro ring resonator (Ali Shahidinejad et al. 2018), Add Drop filter (Joannopoulos et al. 1997a, b; Hsiao and Lee 2009; Mahmoud et al. 2012; Rajasekar and Robinson 2018; Sathyadevaki and Raja 2017; Qiang et al. 2004; Alipour-Banaei et al. 2014a, b; Robinson and Nakkeeran 2018; Rezaee et al. 2018; Rashki and Chabok 2017; Chhipa et al. 2016, Alipour-Banaei et al. 2014a, b; Massoudi et al. 2019) and etc.

One of the important components to work in the Wavelength Division Multiplexing (WDM) system is ADF. The ADF drops the desired wavelength without disturbing the other wavelength in the spectrum. The filter is used in Photonic switches (Beggs et al. 2008), Modulators (Jiang et al. 2005). In the literature survey ADF is reported in Square lattice (Joannopoulos et al. 1997a, b) and Hexagonal lattice (Joannopoulos et al. 1997a, b) using resonant cavity like Hexagonal (Hsiao and Lee 2009) shape, X shape (Mahmoud et al. 2012), Trapezoid shape (Rajasekar and Robinson 2018), Square shape (Sathyadevaki and Raja 2017), Quasi square shape (Qiang et al. 2004; Alipour-Banaei et al. 2014a, b), Circular shape (Robinson and Nakkeeran 2018), H shape (Rezaee et al. 2018), Flower shape (Rezaee et al. 2018), Curved Fabry Perot shape (Rashki and Chabok 2017), Elliptical shape (Chhipa et al. 2016), and Super Elliptical shape (Massoudi et al. 2019).

From the literature survey, it is inferred that most of the ADF are designed using different shapes of the resonant cavity. Many designs provide better performance in dropping efficiency and device size. However, the parameters like Q factor and narrow spectral linewidth are needed to be improved in the ADF to meet the ITU standards for on demand applications like Voice over IP high-speed internet, and High Definition Television (HDTV). Hence, in this paper, a new square shape ring resonator ADF is proposed. The proposed filter is designed to work with constructive interference to obtain the high dropping efficiency, narrow spectral linewidth, and high Q factor at resonance wavelength. The

high Q factor is obtained by increasing the rod between waveguide and cavity (Fan et al. 2002).

Further, the functional parameters of the proposed filters are investigated with respect to the structural parameters to tune the different strong resonant wavelengths to improve the utilization of the device for many applications. The Band gap analysis of the proposed filter before and after the defects are studied with Plane Wave Expansion (PWE) Method (Shi et al. 2004) and the dropping/transfer spectrum analyzed through the Finite Difference Time Domain (FDTD) method (Qiu et al. 2001).

The paper is organized as follows; The Sect. 2 discusses the structural parameter and gap map analysis for the lattice. The proposed design and working principle are discussed in Sect. 3. The Sect. 4 discusses the simulation results of the ADF. Investigation of the tuning mechanism for the ADF is discussed in Sect. 5. Finally, the Sect. 6 concludes the paper.

2 Photonic band gap structure

A semiconductor is a promising material for manufacturing electronic devices due to the presence of Electronic Band Gap. The photonic device emerges due to the existing Photonic Band Gap (PBG) in selected semiconductor material in order to design the optical devices. Nonetheless, these materials should have two properties for optical manipulation such as high refractive index contrast and suitable for nanofabrication.

The proposed ADF is designed with a square lattice array of periodic dielectric rods with high refractive index of 3.19, regular radius of the rod of 130 nm, Period (lattice constant) of 650 nm which results in useful PBG for realizing optical device. The periodic dielectric rods permit the Transverse Electric (TE) wave through which Magnetic field parallel to the rod axis. The proposed filter is designed with the dimension of 35×28 rods in X and Z direction. The PBG before defects is calculated using the PWE and it is given in Fig. 1.

The band diagram of proposed ADF consists of two TE PBGs, first TE PBG normalized frequency in the range of $0.296 < a/\lambda < 0.432$ and its wavelength range between 1504 to 2195 nm, which covers a wide range of optical communication band that are genuinely used for designing optical devices. The second TE band gap varies from $0.746 < a/\lambda < 0.763$

Fig. 1 PBG before introducing the defects

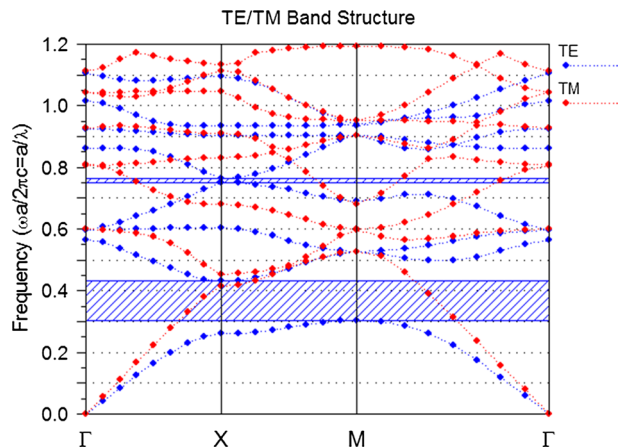


Fig. 2 Effects of normalized frequency with respect to the rod radius

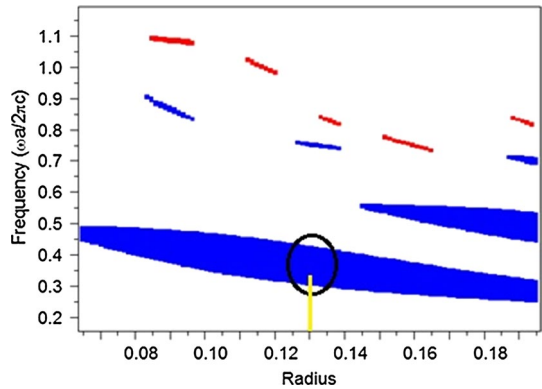
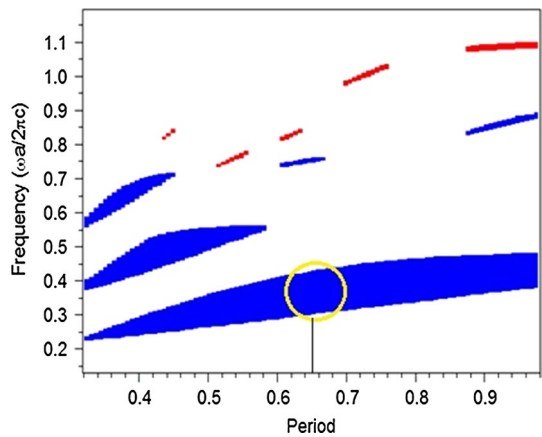


Fig. 3 Effects of normalized frequency with respect to the lattice constant (period)



and corresponding wavelength are 851 nm to 870 nm, which is outside the optical communication window and hence not preferred for the proposed design.

The optimization of structural parameter with respect to normalized frequency is calculated using PWE method. The structural parameters, such as, radius of the rod, lattice constant (period), refractive index (δ) to be optimized in the wavelength range of the optical communication. In the Fig. 2, the optimized rod radius (R) of the proposed filter is 130 nm and lattice constant (a) tuned to 650 nm which is shown in Fig. 3, and refractive index is optimized with 3.19 for the signal of interest as shown in Fig. 4. The guided mode after introducing the defects in the lattice is shown in Fig. 5. At resonance frequency, the resonant wavelength tunneling in the PBG is based on the defects.

3 Rounded square ring resonator based add drop filter

3.1 Basic mechanism

Figure 6 shows the architecture of the WDM network. The four different wavelengths with the spectral linewidth of 0.8 nm arrive from the main office. The SMF is used as medium

Fig. 4 Effects of normalized frequency with respect to the refractive index difference (δ)

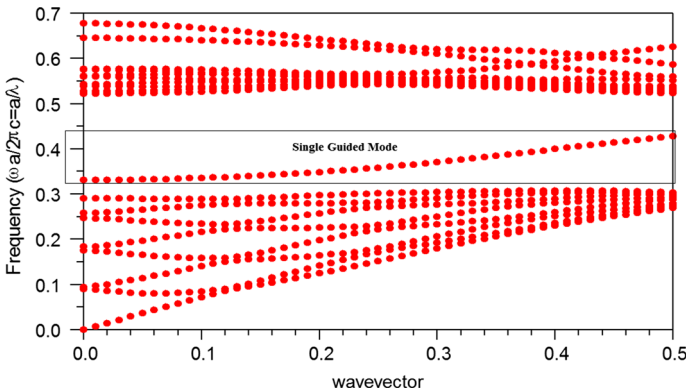
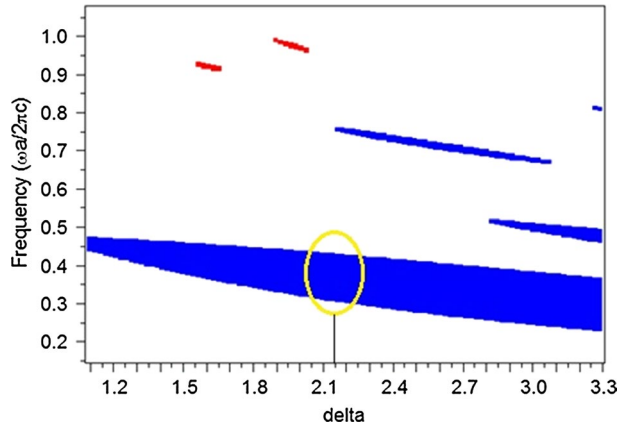


Fig. 5 Band gap diagram after introducing line and point defects

from the main office to transfer the user data to receiver end for the different applications. The ADF is a prominent device in the network to select or drop the desired wavelength to the network without disturbing the other wavelength from the SMF (Park et al. 2004).

ADF plays an important role in fiber communication systems. ADF consists of the four ports, namely, Port A, Port B, Port C and Port D. The Port A is the input port, Port B is a Transmission Port, Port C is a backward drop port, and Port D is a forward drop port. The basic structure of ADF consists of ring resonator and two optical waveguides, resonant cavity slot in between the waveguides. For communication applications, the ADF works in two desirable functions like ON and OFF state. The input Port A allows the WDM signal ($\lambda_1 \lambda_2 \lambda_3 \lambda_4$) (Refer Fig. 6.) in the ADF.

In ON state, unique resonant frequency (λ_1) get resonance inside the cavity, completely (100%) light signal transfer to drop waveguide (Port C) via resonant cavity with the principle of the Photonic Tunneling effect. The signal coupling to drop waveguide based on the structural parameters like regular rod radius, scatterer rods, coupling rods and adjacent rods. The maximum efficiency of light can be transferred from the bus waveguide (Port A) to drop waveguide (Port C) through cavity which should follow the condition $kd = (n + 1/2) \pi$, where; k is the wave vector, n is the integer, and d is

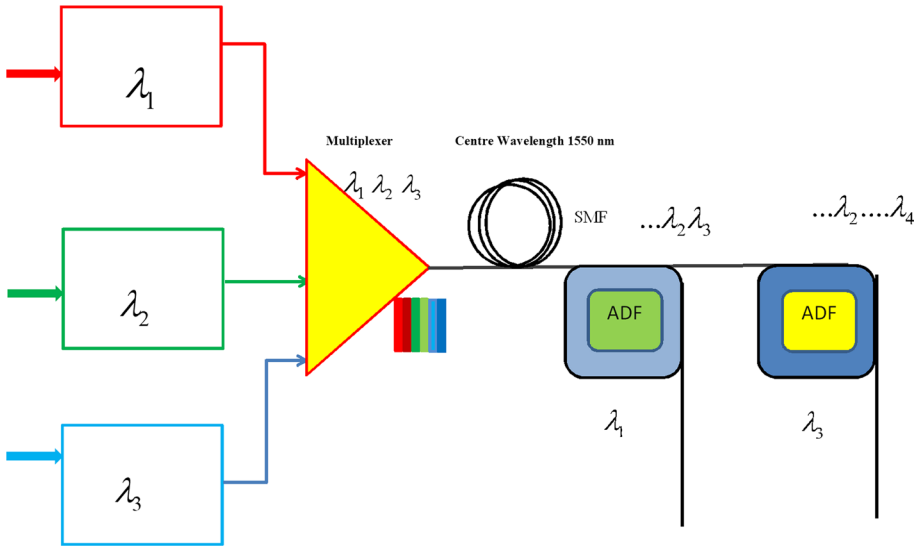
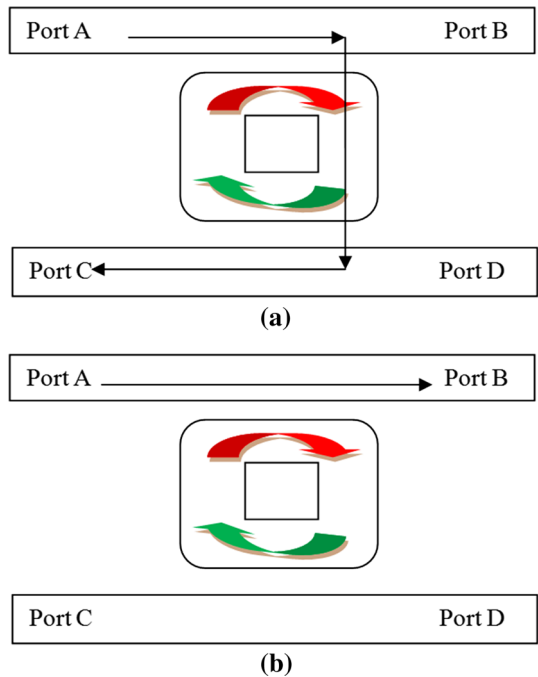


Fig. 6 Schematic representation of WDM network with Add Drop Filter

the distance between the two optical cavities. However, the Transmission Port (Port B) transfers all other wavelengths other than the resonant frequency and zero power transmission in Forward drop (Port D) port which is shown in Fig. 7a. In OFF state, the

Fig. 7 ADF response at a ON state b OFF state



signal is not transferred between the Bus waveguide and drop waveguide. The signal lies in the bus waveguide at Transmission port (Port B) which is shown in Fig. 7b.

3.2 Proposed add drop filter

The proposed RSRR based ADF is shown in Fig. 8. The filter is designed with RSRR with four ports. The line defect is introduced in 2DPC lattice to design bus and drop waveguide. The RSRR allows the electric field waves to build a round trip with the phase shift of 2π for the different waves, which provide constructive interference. The interference in the cavity provides a high resonant peak in certain frequency. The RSRR designed by removing the 9 rods on each side to bring the square shape cavity and 4 scatterer rods in the corner it shapes the rounded shape square cavity. Inner ring is designed with 32 rods and 4 center rods are removed to design quasi square. The entire structure of the structural parameter uses the regular rod radius of 130 nm. The removal of center rod influence to reduce the radiation field scattering, which help to enhance the coupling efficiency to the Port C. The single rod placed at each corner of square act as scatterer rods (R3) which is highlighted in green color. It minimizes the scattering loss, and back and forth reflection waves in order to improve the resonator performance.

The coupling rods (R1) in the outer edge of the square cavity help to couple the photons to drop (Port D) and add (Port B) port which is highlighted in dark black and blue color. The coupling rod radius is important to get higher coupling efficiency and it provides the better confinement of signal to drop waveguide. The coupling rod radius varied from 129 to 133 nm to find the best rod radius with transmission efficiency is shown in Fig. 17.

The coupling rod radius (130 nm) provides the higher dropping efficiency in Port C compare to other rod radius with narrow spectral linewidth of 0.7 nm, and quality factor of 2223. Hence it is considered for the proposed design. Best of our knowledge, this is the

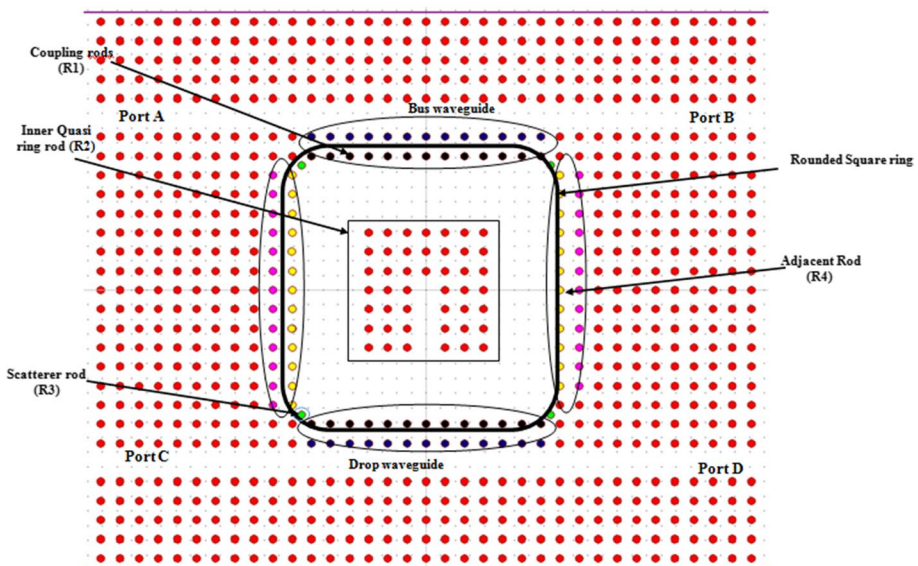


Fig. 8 Proposed rounded square ring resonator based add drop filter

first time to report all structural parameters like adjacent rods, scatterer rods, inner quasi ring rod, and coupling rods are design same as regular rod radius of 130 nm. The regular rod radius of 130 nm optimizes after the several iterations to get the best size to provide the better performance parameters in the proposed ADF and it's easy to fabricate.

4 Simulation results and discussion

The transmission spectrum of the proposed filter is measured based on the received power in the Port B, Port C and Port D. The power monitor place in the receiver port to measure the power based on Finite Difference Time Domain (FDTD) algorithm. The output power measure using the following equation,

$$T(f) = \frac{1/2 \int \text{real}(p(f)^{\text{monitor}})dS}{\text{SourcePower}} \quad (1)$$

where, $T(f)$ denotes the function transmission as function of wavelength, $p(f)$ denotes the pointing vector, and dS denotes the surface normal.

The 2D Finite Difference Time Domain (FDTD) works with the Perfect Matched Layer Absorbed Boundary Condition (PML ABC). The PML ABC is an artificial boundary layer to support the simulation in open boundary condition (Free space), the PML strongly absorbs all the incident waves in all directions, angle without any reflection inside the PC lattice (Chew et al. 1996). The proposed ADF filter uses the PML width of 500 nm, and reflection of 10^{-8} for the best performance.

To work in FDTD, it is important to choose the proper spatial and temporal grid size and time step to match the simulation output with a real time system (Xiao et al. 1993). The proper grid size is calculated using the $a/16=40$ nm and time step of $\Delta t=0.02203$ is used in the FDTD algorithm, it provides stable output and less time leads to oscillation output. The time step calculated by

$$\Delta t \leq \frac{1}{c \sqrt{\frac{1}{\Delta x^2} + \frac{1}{\Delta y^2}}} \quad (2)$$

where Δt denotes the step time, C denotes the speed of light in free space respectively.

The WDM multiplexed signal launched in the input Port A with the center wavelength of 1550 nm. The resonant wavelength (1636.2 nm) is coupled to the resonator with the coupling rods (R1) through the drop waveguide. The resonator gets a peak resonance and drops the output power to Port C and remaining wavelength forward to Port B and a small amount of scattering power transferred to Port D.

Figure 9 shows the normalized output spectrum at the strong wavelength peak at 1636.2 nm in the dropping Port C with the Transmission efficiency of about 100%. The Full Width Half Maximum (FWHM) is 0.7 nm. The efficiency of the filter is calculated using the quality factor (Q). The Q factor is measured by the formula (Ohteru et al. 1993)

$$Q = \frac{\lambda}{\Delta \lambda} \quad (3)$$

where λ is the strong resonant wavelength and $\Delta \lambda$ is spectral linewidth (FWHM) of the resonant wavelength. The proposed ADF drop the wavelength at 1636.2 nm and high quality factor about 2337, which is more suitable for WDM systems.

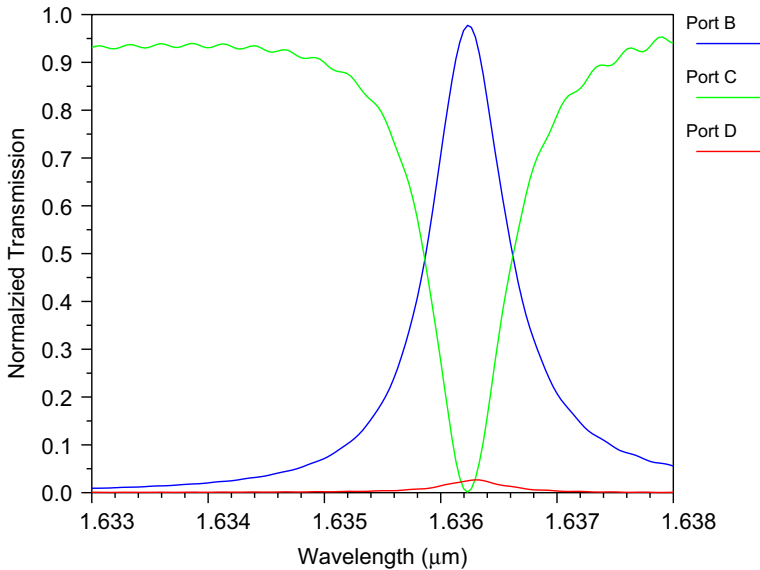


Fig. 9 Normalized output spectrum of the proposed Add Drop filter

The field pattern for backward drop optical power at Port C is shown in Fig. 10. The optical power at the resonant wavelength move towards Port C and other than resonant wavelengths transferred to Port B and no power at Port D. The ADF reduces the complexity of fabrication by reducing the defects. The defects rod radius 130 nm optimize globally after tuning of refractive index, lattice constant, and shape to drop the desired wavelength.

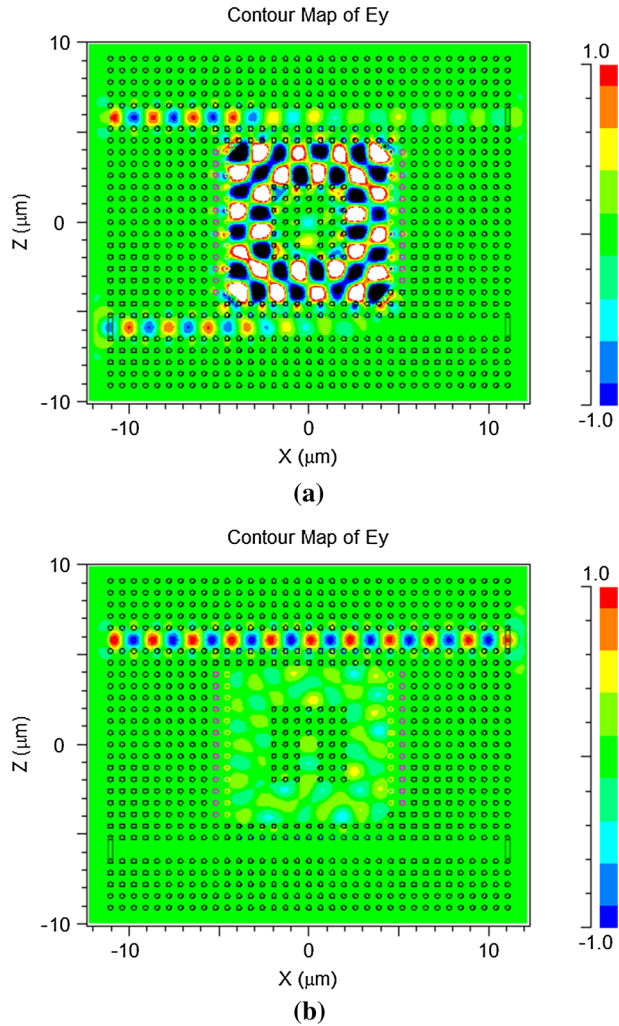
5 Parameters affecting the performance of the ADF

The proposed ADF drops the resonant wavelength at 1636.2 nm with high Q factor to support WDM systems. To broaden the utilization of ADF in real time and on demand applications, tuning mechanism of ADF is investigated by varying the structural parameter and properties like adjacent rods, scatter rods, inner quasi-square rods, periods, coupling rod radius and radius of regular rods. The proposed PBG in the range of $0.292 < a/\lambda < 0.432$, as a structural parameter varies, resonant wavelength from ADF also drops the different resonant wavelength within the PBG. The value of structural parameter is increased propagation of guided mode in ADF shifted in higher wavelength and corresponding strong resonant peak is dropped.

5.1 Lattice constant tuning

Lattice constant of the structure is varied with an increment of 1 nm from 650 to 655 nm to measure the sensitivity of lattice constant with resonant wavelength. The normalized output spectrum for different lattice constant is shown in Fig. 11. From the simulation results, it is observed that strong resonant wavelength of the drop filter is shifted to higher wavelength of 1 nm compared with a reference value of 650 nm also small variation in

Fig. 10 Electric field distribution of the proposed Add Drop filter at **a** ON resonance (1636.2 nm) and **b** OFF resonance (1633 nm)



normalized transmission and spectral linewidth remain constant. Performance parameters of ADF with the variation of lattice constant are given in the Table 1.

$$s_L = \frac{\Delta\lambda}{\Delta\text{Lattice Constant}} = \frac{0.2}{1} = 0.2 \text{ nm} \tag{4}$$

The changes of lattice constant are highly sensitive to resonant wavelength Tuning.

5.2 Effect of adjacent rod radius

In ADF, the reference rod radius of the adjacent rod (R4) is 130 nm. The impact of adjacent rod radius is analyzed by increasing the rod radius with a step value of 1 nm from 131 nm—133 nm by keeping other structural parameters are constant. Figure 12 shows

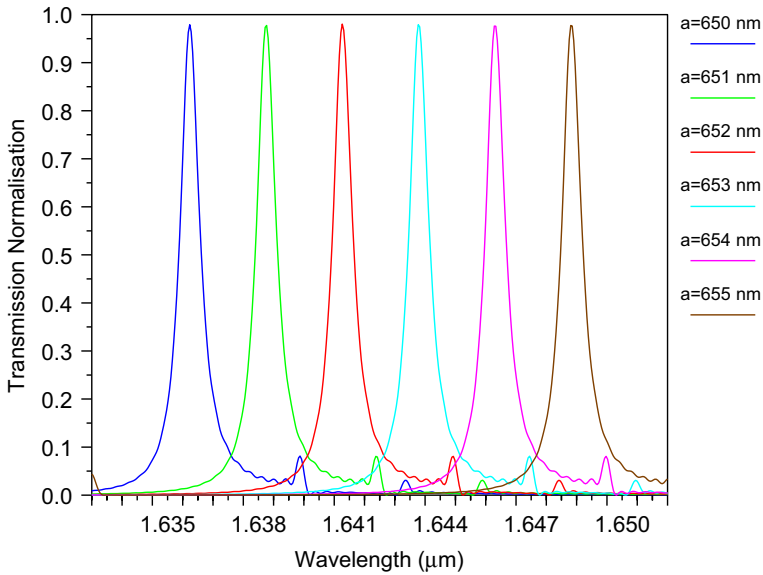


Fig. 11 Output spectrum for different lattice constant

Table 1 Performance parameter with the changes of Lattice constant (a) with performance parameters like resonant wavelength, normalized transmission, spectral linewidth, and quality factor

| S. no. | Lattice constant (nm) | Resonant wavelength (nm) | Normalized transmission (%) | Spectral linewidth (nm) | Quality factor |
|--------|-----------------------|--------------------------|-----------------------------|-------------------------|----------------|
| 1 | 650 | 1630.3 | 97.8 | 0.7 | 2329 |
| 2 | 651 | 1630.5 | 97.4 | 0.7 | 2329 |
| 3 | 652 | 1630.7 | 97.8 | 0.8 | 2038 |
| 4 | 653 | 1630.9 | 97.8 | 0.8 | 2038 |
| 5 | 654 | 1631.1 | 97.6 | 0.7 | 2330 |
| 6 | 655 | 1631.4 | 97.6 | 0.8 | 2039 |

the normalized spectrum for different adjacent rod radius. The performance parameter of R4 is tabulated in Table 2. From the results, strong resonant wavelength shift by 0.3 nm to higher wavelength with correspondingly dropping efficiency and quality factor slightly increased however the spectral linewidth (0.8 nm) remain constant.

Through analyzing the tuning mechanism of different wavelength to the proposed ADF, the sensitivity of the adjacent rod with resonant wavelength is measured from the equation.

$$S_A = \frac{\Delta \lambda}{\Delta R4} = \frac{0.3}{1} \tag{5}$$

The sensitivity of adjacent rod is 0.3 resonant wavelengths tuning is highly sensitive to changes of adjacent rod and it's important to observe spectral linewidth and Normalized transmission remain constant.

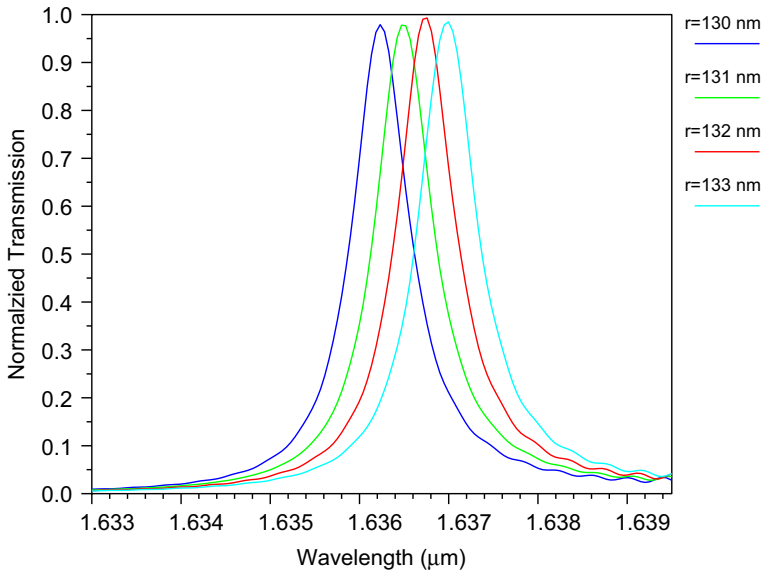


Fig. 12 Effect of change of output spectrum adjacent rod radius

Table 2 Performance parameter with the changes of adjacent rod radius (R4) with performance parameters like resonant wavelength, normalized transmission, spectral linewidth, and quality factor

| S. no. | R4 (nm) | Resonant wavelength (nm) | Normalized transmission (%) | Spectral linewidth (nm) | Quality factor |
|--------|---------|--------------------------|-----------------------------|-------------------------|----------------|
| 1 | 130 | 1636.0 | 98 | 0.8 | 2045 |
| 2 | 131 | 1636.5 | 98.0 | 0.8 | 2045.65 |
| 3 | 132 | 1636.8 | 99.2 | 0.8 | 2046 |
| 4 | 133 | 1637.1 | 98.4 | 0.8 | 2046.37 |

5.3 Scatterer rod tuning

In ADF, the reference rod radius of the scatterer rod (R3) is 130 nm. Scatterer rods are placed at each corner of four sides in the square ring resonator. The scatterer rod reduces the scatter loss and reflection waves from the rod improve the resonator performance. The impact of scatterer rod tuning with respect to the resonant wavelength is studied. The scatterer rod of the proposed ADF is varied with an increment of 1 nm from 130 to 132 nm and the corresponding output spectrum of different scatterer rod radius is investigated which is shown Fig. 13. From the simulation results, it observed that peak resonant wavelength shifted by 0.1 nm from the reference wavelength. The dropping efficiency and quality factor is slight change and spectral linewidth remain constant and is observed by changing scattered rod.

The sensitivity of scatterer rod is defined as a resonant wavelength variation with the scatterer rod variation $\Delta\lambda/\Delta R3$, sensitivity calculated as ± 0.2 nm/1 nm. The performance parameter of R3 is tabulated in Table 3.

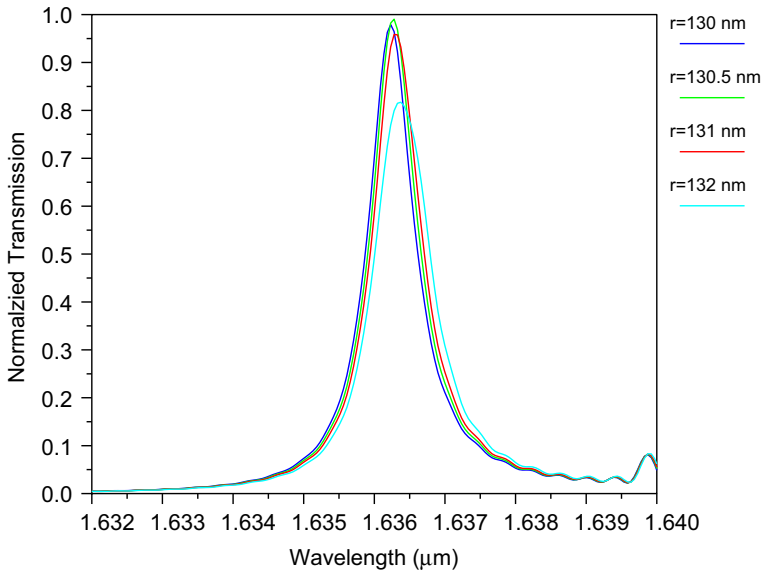


Fig. 13 Output spectrum for different scattered rod radius

Table 3 Functional parameter with the changes of Scatterer rod radius (R3) with performance parameters like resonant wavelength, normalized transmission, spectral linewidth, and quality factor

| S. no. | R3 (nm) | Resonant wavelength (nm) | Normalized transmission (%) | Spectral linewidth (nm) | Quality factor |
|--------|---------|--------------------------|-----------------------------|-------------------------|----------------|
| 1 | 130 | 1636.0 | 99.0 | 0.7 | 2337.0 |
| 2 | 130.5 | 1636.2 | 99.0 | 0.8 | 2045.25 |
| 3 | 131 | 1636.3 | 95.76 | 0.8 | 2045.37 |
| 4 | 132 | 1636.4 | 81.61 | 0.8 | 2045.5 |

5.4 Coupling rod radius tuning

In ADF, the reference rod radius of coupling rod radius (R1) is 130 nm. This rod optimizes with a radius of 130 nm, it is used to couple the incoming light from the bus waveguide to drop waveguide through rounded RSRR. Two rows of rods used for coupling to provide better coupling light to the resonator. To analyze the impact of variation with coupling rods, the coupling rod radius is varied from 130 nm-133 nm with 1 nm shift. It is observed that the resonant wavelength is not shifted, however, there is a trivial decrement of transmission efficiency is observed for rod radius other than reference rod (130 nm) which is shown in Fig. 14. The tuning mechanism in the ADF filter and coupling rod radius to be fixed as 130 nm, however, the other structural parameters are varied in order to drop different resonant wavelengths. The performance parameter of Radius 1 is tabulated in Table 4. The sensitivity of Scatterer rod is defined as a resonant wavelength variation with the scatterer rod variation $\Delta\lambda/\Delta R1$, sensitivity in the ratio of 0 nm/1 nm.

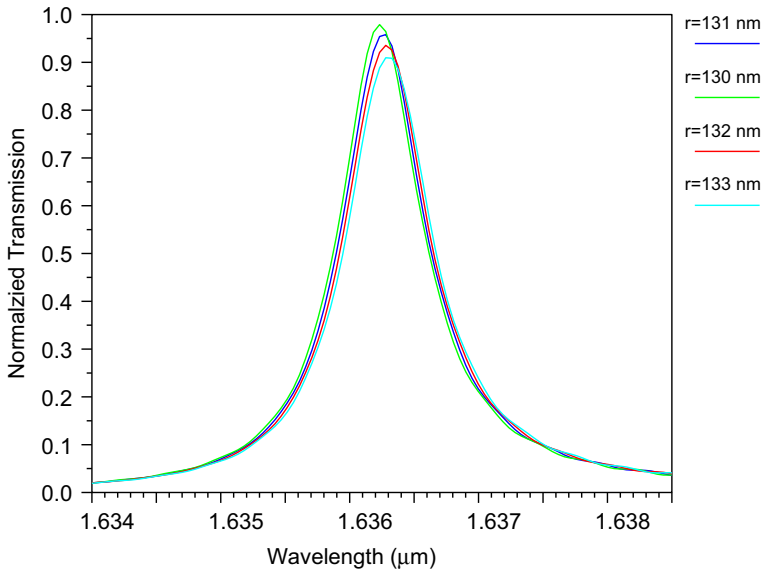


Fig. 14 Output spectrum for different coupling rod radius

Table 4 Performance parameter with the changes of coupling rod radius (R1) with performance parameters like resonant wavelength, normalized transmission, spectral linewidth, and quality factor

| S. no. | R1 (nm) | Resonant wavelength (nm) | Normalized transmission (%) | Spectral linewidth (nm) | Quality factor |
|--------|---------|--------------------------|-----------------------------|-------------------------|----------------|
| 1 | 131 | 1636.3 | 95 | 0.8 | 2045 |
| 2 | 132 | 1636.3 | 93 | 0.8 | 2045 |
| 3 | 133 | 1636.3 | 90 | 0.8 | 2045 |

5.5 Regular rod radius Tuning

Sensitivity of the regular rod tuning is measured by the ratio of difference in resonance wavelength by changing in the rod radius of regular rod. The rod radius varied from 129 to 131 nm with increment of 0.5 nm, it is observed that resonant wavelength is shifted to higher wavelength of 0.6 nm for every increasing of 0.5 nm rod radius, which is shown Fig. 15. It is also observed that abrupt variation in Transmission Efficiency and quality factor, but spectral linewidth remain constant. The sensitivity of Radius 5 rod variation is measured by

$$S_{Radius} = \frac{\Delta\lambda}{\Delta Radius} = \frac{0.6}{0.5} = 1.2 \text{ nm} \tag{6}$$

The Radius of the regular rod is highly sensitive to resonant wavelength Tuning. The performance parameter of Radius 1 is tabulated in Table 5.

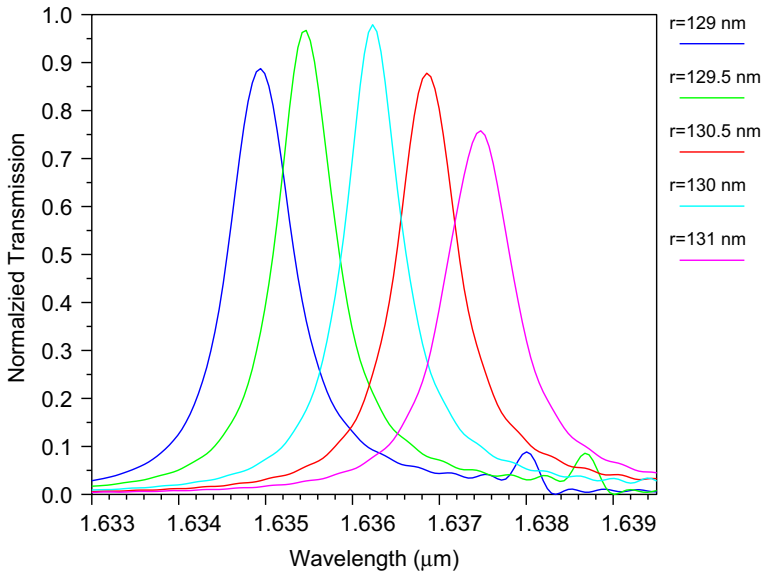


Fig. 15 Output spectrum for different coupling rod radius

Table 5 Performance parameter with the changes of regular rod (Radius) with performance parameters like resonant wavelength, normalized transmission, spectral linewidth, and quality factor

| S. no. | Radius (nm) | Resonant wavelength (nm) | Normalized transmission (%) | Spectral linewidth (nm) | Quality factor |
|--------|-------------|--------------------------|-----------------------------|-------------------------|----------------|
| 1 | 129 | 1634.9 | 88.7 | 0.9 | 1816 |
| 2 | 129.5 | 1635.5 | 96.3 | 0.8 | 2044 |
| 3 | 130 | 1636 | 99 | 0.8 | 2045 |
| 4 | 130.5 | 1636.9 | 87.66 | 0.8 | 2046 |
| 5 | 131 | 1637.5 | 75.45 | 0.8 | 2046.87 |

5.6 Inner rod tuning

In ADF, the reference rod radius of the inner quasi ring rod radius (R2) is 130 nm, to measure sensitivity, the inner rod radius varied from 128 to 131 nm with the increment of 1 nm and normalized spectrum is shown in Fig. 16. From the results, it is noticed that the abrupt changes in the performance parameter like dropping efficiency, spectral linewidth, and quality factor.

The performance parameter of ADF with different inner ring rod radius is tabulated in Table 6. However, changing the inner rod radius result in uneven output of the filter; it leads to more changes in transmission efficiency, spectral linewidth, and Q factor. Changing the inner rod radius for tuning mechanism is not feasible in the proposed filter due its uncertainty in the output.

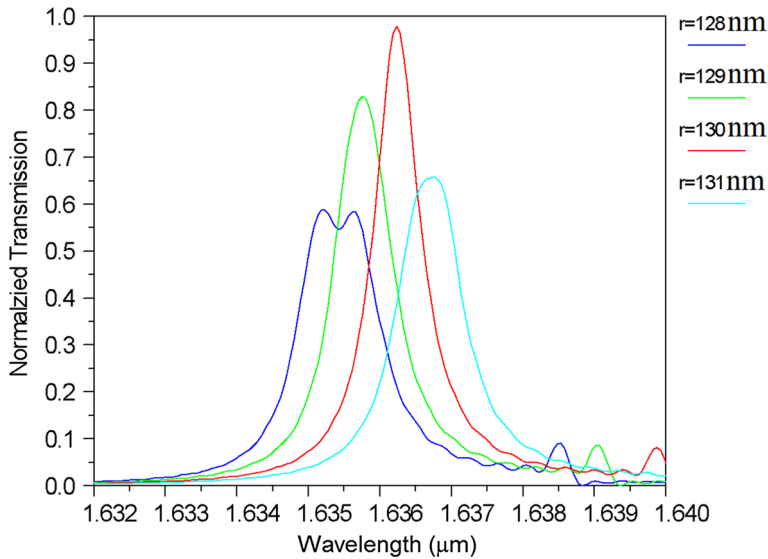


Fig. 16 Output spectrum for different inner quasi ring rod radius

Table 6 Performance parameter with the changes of inner quasi ring rod radius with performance parameters like resonant wavelength, normalized transmission, spectral linewidth, and quality factor

| S. no. | Radius (nm) | Resonant wavelength (nm) | Normalized transmission (%) | Spectral linewidth (nm) | Quality factor |
|--------|-------------|--------------------------|-----------------------------|-------------------------|----------------|
| 1 | 128 | 1635.2 | 58.5 | 2.1 | 778 |
| 2 | 129 | 1635.8 | 82.6 | 1 | 1635 |
| 3 | 130 | 1636 | 99 | 1 | 1636 |
| 4 | 131 | 1636.8 | 65.6 | 1.1 | 1488 |

5.7 Effect of variation in refractive index of rods

Tuning to the desired wavelength based on input parameter is an important property in ADF. The performance of ADF is validated for refractive index variation of adjacent rods, corner rods, coupling rods and inner rods. One row of the adjacent rods, coupling rods, inner rods and corner rods are considered to vary at a time in the value of refractive index, while the other rods value unchanged, in every simulation. The output spectra of our proposed design at port D for different values of refractive index of adjacent rods, coupling rods, inner rods and corner rods shown in Figs. 17, 18, 19 and 20. The output wavelengths shift toward higher wavelengths range, with the refractive index from 3.19 to 3.23. The sensitivity of adjacent rods is 0.2/0.01, the shift is accompanied by higher normalized transmission shown in Table 7. The sensitivity of corner rods is 0.1/0.01, the shift is noticed with higher normalized transmission shown in Table 8. The sensitivity of coupling rods and inner rods is 0.2/0.01, while varying the refractive

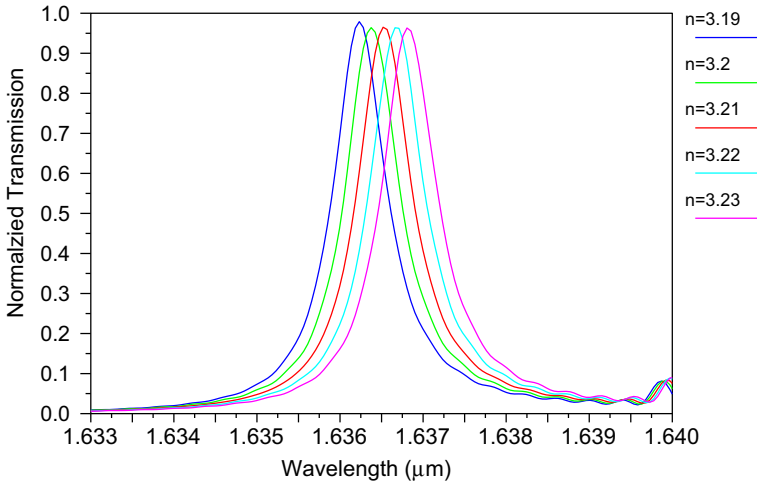


Fig. 17 Output spectra of our proposed design for different values of refractive index of adjacent rods

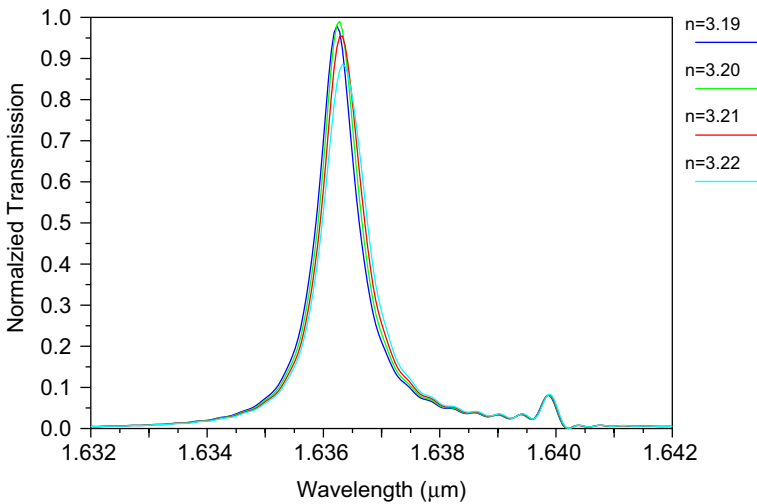


Fig. 18 Output spectra of our proposed design for different values of refractive index of corner rods

index in inner rods and coupling rods trivial decrement in transmission efficiency shown in Tables 9, 10.

The performance parameter of the proposed design is determined by varying the input parameters for different step increments of the input variable and the output spectrum are predicted. Furthermore, the error between the target output value and obtained wavelength is also examined. The flowchart for the proposed design is shown in Fig. 21. The input variable is incremented with different sets in order to predict the targeted resonant wavelength and to calculate the error between the target wavelength and output

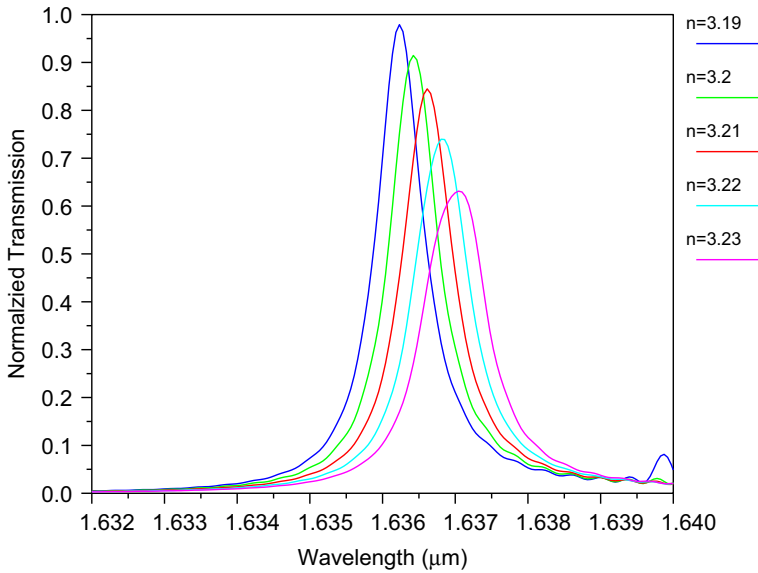


Fig. 19 Output spectra of our proposed design for different values of refractive index of coupling rods

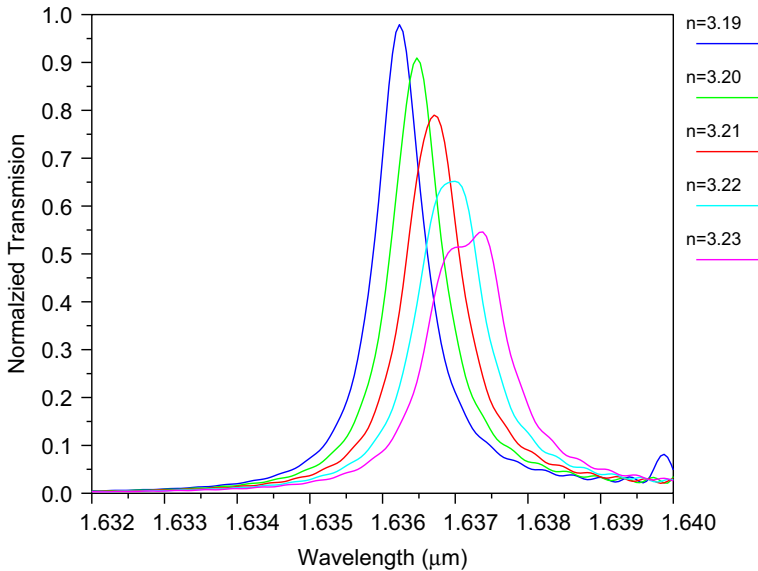


Fig. 20 Output spectra of our proposed design for different values of refractive index of inner rods

wavelength for the different input value. If an error exists between the target and output value, another input value is to be chosen under iteration to select the optimum rod radii with the lattice constant. If no error, then value is predicted and corresponding wavelength is obtained.

Table 7 Performance parameter with the changes of refractive index of adjacent rods with performance parameters like resonant wavelength, normalized transmission, spectral linewidth, and quality factor

| S. no. | n | Resonant wavelength (nm) | Normalized transmission (%) | Spectral linewidth (nm) | Quality factor |
|--------|------|--------------------------|-----------------------------|-------------------------|----------------|
| 1 | 3.19 | 1636.2 | 98 | 0.8 | 2045.25 |
| 2 | 3.20 | 1636.4 | 96.3 | 0.8 | 2045.5 |
| 3 | 3.21 | 1636.5 | 96.4 | 0.8 | 2045.75 |
| 4 | 3.22 | 1636.7 | 96.2 | 0.8 | 2046.00 |
| 5 | 3.23 | 1636.8 | 96.2 | 0.8 | 2045.25 |

Table 8 Performance parameter with the changes of refractive index of corner rods with performance parameters like resonant wavelength, normalized transmission, spectral linewidth, and quality factor

| S. no. | n | Resonant wavelength (nm) | Normalized transmission (%) | Spectral linewidth (nm) | Quality factor |
|--------|------|--------------------------|-----------------------------|-------------------------|----------------|
| 1 | 3.19 | 1636.2 | 98 | 0.8 | 2045.25 |
| 2 | 3.20 | 1636.3 | 99 | 0.8 | 2045.37 |
| 3 | 3.21 | 1636.3 | 95 | 0.8 | 2045.37 |
| 4 | 3.22 | 1636.3 | 88 | 0.8 | 2045.37 |
| 5 | 3.23 | 1636.4 | 65 | 0.8 | 2045.5 |

The tuning range in the proposed ADF achieved from the range of 1536–1637 nm by varying the one of the structural parameters. The tuning of resonant wavelength for novel RSRR is theoretically investigated by altering the structural parameters and the few results are reported hereshown in Table 11.

1. For 1 nm changes in adjacent rod, 0.3 nm resonant wavelength is shifted and 0.8 nm spectral linewidth is observed.
2. For 1 nm changes in scatterer rod, 0.1 nm resonant wavelength is shifted and 0.8 nm stable spectral linewidth is observed.
3. For 1 nm changes in coupling rod, resonant wavelength is not shifted from reference wavelength 1636.2 nm.
4. For 0.5 nm changes in regular rod, 0.6 nm resonant wavelength is shifted from reference wavelength (1636.2 nm) and stable spectral linewidth is observed.
5. For 10 nm change in lattice constant, 25 nm resonant wavelength shift is observed and spectral linewidth is constant.
6. For 1 nm changes in inner quasi ring rods, uncertainty in all performance parameters is observed.

The functional parameters of the filter like lattice, cavity design, backdrop efficiency, spectral linewidth, device size, quality factor, refractive index, and resonant wavelength are compared with reported ADF is tabulated.

In the literature, so far, there are many ring resonator based Add drop filter, such as Hexagonal shape, X shape, Trapezoid shape, Square shape, Quasi square shape, Circular shape,

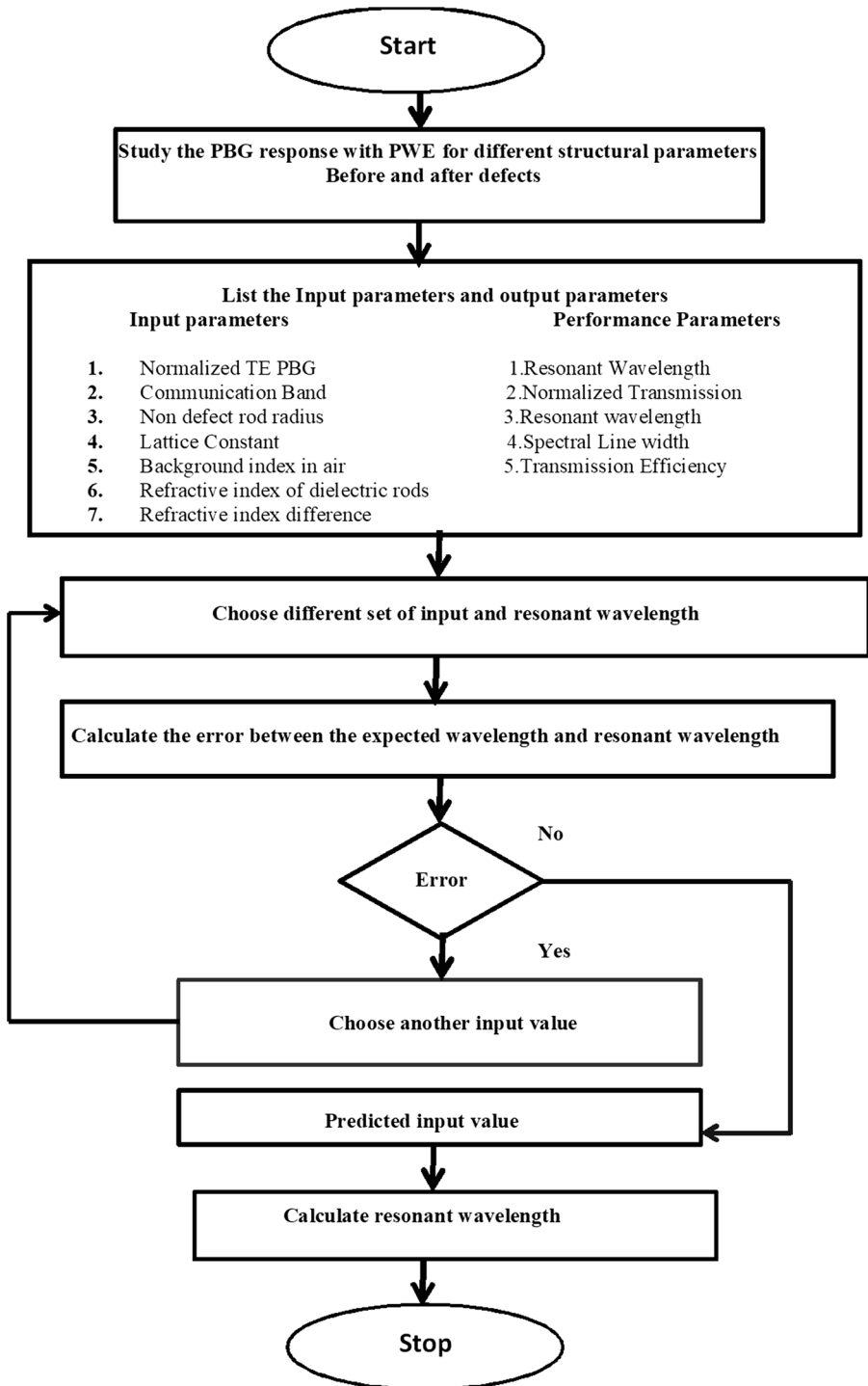


Fig. 21 Flowchart of Photonics parameter optimization

Table 9 Performance parameter with the changes of refractive index of coupling rods with performance parameters like resonant wavelength, normalized transmission, spectral linewidth, and quality factor

| S. no. | n | Resonant wavelength (nm) | Normalized transmission (%) | Spectral linewidth (nm) | Quality factor |
|--------|------|--------------------------|-----------------------------|-------------------------|----------------|
| 1 | 3.19 | 1636.2 | 98 | 0.8 | 2045.25 |
| 2 | 3.2 | 1636.4 | 91 | 0.8 | 2045.50 |
| 3 | 3.21 | 1636.6 | 84 | 0.8 | 2045.75 |
| 4 | 3.22 | 1636.8 | 74 | 0.8 | 2046.00 |
| 5 | 3.23 | 1637 | 63 | 0.9 | 1815.55 |

Table 10 Performance parameter with the changes of refractive index of inner rods with performance parameters like resonant wavelength, normalized transmission, spectral linewidth, and quality factor

| S. no. | n | Resonant wavelength (nm) | Normalized transmission (%) | Spectral linewidth (nm) | Quality factor |
|--------|------|--------------------------|-----------------------------|-------------------------|----------------|
| 1 | 3.19 | 1636.2 | 98 | 0.8 | 2045.25 |
| 2 | 3.2 | 1636.5 | 91 | 0.8 | 2045.62 |
| 3 | 3.21 | 1636.7 | 78 | 0.8 | 2045.87 |
| 4 | 3.22 | 1637 | 65 | 0.9 | 1818.00 |
| 5 | 3.23 | 1637.4 | 54 | 0.9 | 1819.33 |

H shape, Flower shape, Curved Fabry–Perot shape, Elliptical shape, and Super Elliptical shape, are reported for WDM applications. And the primary performance parameters of the ADF, namely, transmission efficiency, Q factor, narrow spectral linewidth and device size are accounted. The parameters like Q factor and narrow spectral linewidth need the improvement in the ADF to meet the ITU standards for on demand applications like Voice over IP high-speed internet, and High Definition Television (HDTV). In order to meet the above demand, in this attempt, a new rounded square shape ring resonator based ADF is proposed, designed and the functional parameters are investigated elaborately.

Best of our knowledge, this is the first time, in the proposed ADF all structural parameters like adjacent rods, scatterer rods, inner quasi ring rod, and coupling rods are same as regular rod radius of 130 nm. The regular rod radius of 130 nm is optimized after the several iterations to get the best size to provide better performance parameters in the proposed ADF and it is easy to fabricate. In addition, the shape of the inner rod is also changed and the functional parameters are studied. Since, square inner rod with rounded square outer rod based ADF provides better performance, it is considered here. The proposed ADF provides 99% of dropping efficiency, narrow spectral linewidth of 0.7 nm, and the Q factor of 2223 with the size of $412.76\mu\text{m}^2$. The functional parameters of the proposed ADF are highly suitable for the implementation of Photonic Integrated Circuits.

Table 11 Lattice type, shape of the cavity, backward efficiency, spectral linewidth, device size, refractive index, and resonant wavelength of the proposed ADF is compared with different lattice

| References | Lattice | Cavity shape | Add/drop (%) | ($\Delta\lambda$) | Device Size (μm^2) | Q factor | $\Delta n/\lambda_0$ |
|----------------------------------|-----------|-----------------------------------------|--------------|---------------------|---------------------------------|----------|----------------------|
| Hsiao and Lee (2009) | Hexagonal | Hexagonal | 55 | 4 | – | 423 | 3.46/1564 |
| Mahmoud et al. (2012) | | X shape | 100 | 4 | – | 377 | 3.46/1550 |
| Rajasekar and Robinson (2018) | | Trapezoid | 100 | 3 | 117.6 | 514 | 3.46/1543 |
| Sathyadevaki and Raja (2017) | | Square | 35 | 3.5 | 280 | 437 | 3.46/1558 |
| Qiang et al. (2007) | Square | Quasi square | 90 | 4 | 242.4 | 387 | 3.46/1531 |
| Alipour-Banaei et al. (2014a, b) | | | 96 | 9.8 | – | 160 | 3.59/1551 |
| Robinson and Nakkeeran (2018) | | Circular | 89 | 3.5 | 173.42 | 399 | 4/1489 |
| Rezaee et al. (2015) | | H shape | 100 | 7 | – | 221 | 4.1/1550 |
| Rashki and Chabok (2017) | | Flower | 100 | 8 | 152.76 | 205.5 | 3.46/1644 |
| Chhipa et al. (2006) | | Curved Fabry Perot | 99 | 13 | 123 | 194 | 3.40/1511 |
| Alipour-Banaei et al. (2014a, b) | | Elliptical resonant ring | 100 | 2 | – | 647 | 4.2/1555 |
| Radhouene et al. | | Square ring (Super elliptic inner ring) | 92 | 0.7 | – | 2210 | 3.19/1547.3 |
| Proposed Work | | Square (Inner quasi ring) | > 98 | 0.7 | 412.76 | 2337 | 3.19/1636.2 |

η backward drop efficiency, Q quality factor, λ_0 strong resonant wavelength, $\Delta\lambda$ spectral linewidth, Δ Delta

6 Conclusion

The proposed Rounded Square Ring Resonator (RSRR) based ADF is designed to support the WDM system to drop the strong resonant wavelength of 1636.2 nm. The novelty in the proposed ADF is to drop the desired wavelength with globalized defect rod radius. The spectral linewidth is 0.7 nm, quality factor is 2337 and transmission efficiency is about 100%. We investigated the effect of structural parameters with resonant wavelength and the best structural parameter for the tuning mechanism is reported. Compared to existing works this ADF offers high narrow linewidth to support DWDM applications and the size is 412.76 μm^2 . Hence, the proposed ADF is suitable for the implementation of Photonic Integrated Circuits (PIC) for DWDM applications. In future, this proposed ADF can be devised to enhance the linewidth to 0.4 nm/0.2 nm/0.1 nm to support DWDM systems.

References

- Alipour-Banaei, H., Mehdizadeh, F., Hassangholizadeh-Kashtiban, M.: A new proposal for PCRR-based channel drop filter using elliptical rings. *Phys. E Low Dimens. Syst. Nanostruct.* **56**, 211–215 (2014b)
- Alipour-Banaei, H., Jahanara, M., Mehdizadeh, F.: T-shaped channel drop filter based on photonic crystal ring resonator. *Optik* **125**(18), 5348–5351 (2014a)
- Balaji, V.R., Murugan, M., Robinson, S.: Optimization of DWDM demultiplexer using regression analysis. *J. Nanomater.* 1–10 (2016)
- Beggs, D.M., White, T.P., O’Faolain, L., Krauss, T.F.: Ultracompact and low-power optical switch based on silicon photonic crystals. *Opt. Lett.* **33**(2), 147–149 (2008)
- Chew, W.C., Liu, Q.H.: Perfectly matched layers for elastodynamics: a new absorbing boundary condition. *J. Theor. Comput. Acoust.* **4**(04), 341–359 (1996)
- Chhipa, M.K., Radhouene, M., Dikshit, A., Robinson, S., Suthar, B.: Novel compact optical channel drop filter for CWDM optical network applications. *Int. J. Photonics Opt. Technol* **2**(4), 26–29 (2016)
- Fan, S., Villeneuve, P.R., Joannopoulos, J.D., Haus, H.A.: Channel drop filters in photonic crystals. *Opt. Express* **3**(1), 4–11 (1998)
- Fan, S., Wang, Z., Miller, D.A., Villeneuve, P.R., Haus, H.A., Joannopoulos, J.D.: Photonic crystal for communication applications. *Active Passive Opt. Comp. WDM Commun. II* **4870**, 339–347 (2002)
- Fenzl, C., Hirsch, T., Wolfbeis, O.S.: Photonic crystals for chemical sensing and biosensing. *Angew. Chem. Int.* **53**(13), 3318–3335 (2014)
- Hsiao, F.L., Lee, C.: A nano-ring resonator based on 2-D hexagonal-lattice photonic crystals. In: 2009 IEEE/LEOS International Conference on Optical MEMS and Nanophotonics, p. 107–108 (2009)
- Jiang, Y., Jiang, W., Gu, L., Chen, X., Chen, R.T.: 80-micron interaction length silicon photonic crystal waveguide modulator. *Appl. Phys. Lett.* **87**(22), 221105-1 (2005)
- Joannopoulos, J.D., Villeneuve, P.R., Fan, S.: Photonic crystals. *Solid State Commun.* **102**(2–3), 65 (1997a)
- Joannopoulos, J.D., Villeneuve, P.R., Fan, S.: Photonic crystals: putting a new twist on light. *Nature* **386**(6621), 143–149 (1997b)
- Kersey, A.D., Berkoff, T.A., Morey, W.W.: Multiplexed fiber Bragg grating strain–sensor system with a fiber Fabry–Perot wavelength filter. *Opt. Lett.* **18**(16), 1370–1372 (1993)
- Mahmoud, M.Y., Bassou, G., Taalbi, A., Chekroun, Z.M.: Optical channel drop filters based on photonic crystal ring resonators. *Opt. Commun.* **285**(3), 368–372 (2012)
- Massoudi, R., Najjar, M., Mehdizadeh, F., Janyani, V.: Investigation of resonant mode sensitivity in PhC based ring resonators. *Opt. Quantum Electron* **51**(3), 1–12 (2019)
- Mehdizadeh, F., Soroosh, M., Alipour-Banaei, H.: Proposal for 4-to-2 optical encoder based on photonic crystals. *IET Optoelectron.* **11**(1), 29–35 (2016)
- Meier, M., Mekis, A., Dodabalapur, A., Timko, A., Slusher, R.E., Joannopoulos, J.D., Nalamasu, O.: Laser action from two-dimensional distributed feedback in photonic crystals. *Appl. Phys. Lett.* **74**(1), 7–9 (1999)
- Ohteru, S., Takachio, N.: Optical signal quality monitor using direct Q-factor measurement. *IEEE Photon. Technol. Lett.* **11**(10), 1307–1309 (1999)

- Park, S.J., Lee, C.H., Jeong, K.T., Park, H.J., Ahn, J.G., Song, K.H.: Fiber-to-the-home services based on wavelength-division-multiplexing passive optical network. *J. Light. Technol.* **22**(11), 2582–2591 (2004)
- Qiang, Z., Zhou, W., Soref, R.A.: Optical add-drop filters based on photonic crystal ring resonators. *Opt. Express* **15**(4), 1823–1831 (2007)
- Qiu, M.: Analysis of guided modes in photonic crystal fibers using the finite-difference time-domain method. *Microw. Opt. Technol. Lett.* **30**(5), 327–330 (2001)
- Rajasekar, R., Robinson, S.: Trapezoid 2D photonic crystal nanoring resonator-based channel drop filter for WDM systems. *Photonic Netw. Commun.* **36**(2), 230–245 (2018)
- Rashki, Z., Chabok, S.J.S.M.: Novel design of optical channel drop filters based on two-dimensional photonic crystal ring resonators. *Opt. Commun.* **395**, 231–235 (2017)
- Rayleigh, L.: XVII. On the maintenance of vibrations by forces of double frequency, and on the propagation of waves through a medium endowed with a periodic structure. *Philos. Mag.* **24**(147), 145–159 (1887)
- Rezaee, S., Zavvari, Alipour-Banaei, H.: A novel optical filter based on H-shape photonic crystal ring resonators. *Optik* **126**(20), 2535–3538 (2015)
- Robinson, S., Nakkeeran, R.: Two dimensional photonic crystal ring resonator based add drop filter for CWDM systems. *Optik* **124**(18), 3430–3435 (2018)
- Sathyadevaki, R., Raja, A.S.: Photonic crystal-based optical filter: a brief investigation. *Photonic Netw. Commun.* **33**(1), 77–84 (2017)
- Shahidinejad, A.: Soliton pulse generation for WDM-based free space optics communication using microring resonators. *J. Opt. Commun.* **25**(1), 59–64 (2018)
- Shi, S., Chen, C., Prather, W.: Plane-wave expansion method for calculating band structure of photonic crystal slabs with perfectly matched layers. *J. Opt. Soc. Am. A* **21**(9), 1769–1775 (2004)
- Sun, S.: A dual-band bandpass filter using a single dual-mode ring resonator. *IEEE Microw. Wirel. Compon. Lett.* **21**(6), 298–300 (2011)
- Tran, A.T.T.D., Lo, Y.H., Zhu, Z.H., Haronian, D., Mozdy, E.: Surface micromachined Fabry–Perot tunable filter. *IEEE Photonics Technol. Lett.* **8**(3), 393–395 (1996)
- Wooten, E.L., Stone, R.L., Miles, E.W., Bradley, E.M.: Rapidly tunable narrowband wavelength filter using LiNbO₃/sub 3/unbalanced Mach–Zehnder interferometers. *J. Light. Technol.* **14**(11), 2530–2536 (1996)
- Xiao, S., Vahldieck, R.: An efficient 2-D FDTD algorithm using real variables (guided wave structure analysis). *IEEE Microw. Wirel. Compon. Lett.* **3**(5), 127–129 (1993)
- Zhang, Y., Zhang, Y., Li, B.: Optical switches and logic gates based on self-collimated beams in two-dimensional photonic crystals. *Opt. Express* **15**(15), 9287–9292 (2007)

Publisher's Note Springer Nature remains neutral with regard to jurisdictional claims in published maps and institutional affiliations.

Authors and Affiliations

Massoudi Radhouene¹ · V. R. Balaji²  · Monia Najjar^{1,3} · S. Robinson⁴ · Vijay Janyani⁵ · M. Murugan⁶

¹ National Engineering School of Tunis Communications Systems LR-99-ES21 (LR-Sys'Com-ENIT), University of Tunis El Manar, 1002 Tunis, Tunisia

² School of Electronics Engineering, Vellore Institute of Technology, Vandalur - Kelambakkam Road, Chennai, Tamil Nadu 600 127, India

³ University of Tunis El Manar, Higher Institute of Computer, 2080 Ariana, Tunisia

⁴ Mount Zion College of Engineering and Technology, Pudukkottai, Tamil Nadu 622 507, India

⁵ Department of Electronics and Communication Engineering, Malaviya National Institute of Technology, Jaipur, India

⁶ SRM Valliammai Engineering College, Kattankulathur 603203, Tamilnadu, India